


Significance and Sensor Utility of Phase in Quantum Localization Transition

Kunal K. Das

Department of Physical Sciences, Kutztown University of Pennsylvania, Kutztown, Pennsylvania 19530, USA
and Department of Physics and Astronomy, State University of New York, Stony Brook, New York 11794-3800, USA

 (Received 3 February 2020; accepted 28 July 2020; published 13 August 2020)

The degree of localization of the Harper-Hofstadter model is shown to display striking periodic dependence on phase degrees of freedom, which can depend on the nature of the boundary condition, reminiscent of the Aharonov-Bohm effect. In the context of implementation in a finite ring-shaped lattice structure, this phase dependence can be utilized as a fundamentally different principle for precision sensing of rotation and magnetic fields based on localization rather than on interferometry.

DOI: 10.1103/PhysRevLett.125.070401

Phase is a defining feature of quantum mechanics, yet some of its most profound effects were initially overlooked, notably the Aharonov-Bohm effect [1], the physical relevance of the geometric phase [2], and the Josephson effect [3]. Here we reexamine the much-studied Harper-Hofstadter [4,5] model to find that its inherent phase degrees of freedom can have a striking observable influence on its characteristic localization transition, and we discuss how those effects could be harnessed as a new principle for precision sensing of rotation and magnetic fields. We present evidence based on simulations using multiple approaches and provide arguments for the origins of these effects, while identifying the circumstances under which they gain physical relevance.

The Harper equation is deceptively simple to represent,

$$J_1[\psi_{n+1} + \psi_{n-1}] + J_2 \cos(2\pi\alpha n + \theta)\psi_n = E\psi_n, \quad (1)$$

yet encompasses a wealth of mathematical features and physical significance. Since 1955, when Harper used it to describe electrons in a 2D periodic lattice subject to a magnetic field [4], this equation has been the subject of countless studies, many highly consequential [5–7], augmented in recent years by the equation's relevance for synthetic gauge structures in ultracold atoms [8–11]. Certain trends, however, have persisted that will be reexamined here, specifically, the phase θ has been primarily relevant as relic of the extra translational degree of freedom of the 2D model [12,13], the periodicity associated with rational α is seldom interpreted in terms of a physical 1D ring, and the overarching interest has been driven by fundamental physics rather than applications.

Discrete model.—The Hamiltonian in Eq. (1) lacks periodicity for irrational α , but for rational values $\alpha = p/q$ with $p, q, \in [1, 2, \dots]$ and where p and q are coprimes, it has period q and can be realized in a ring-shaped lattice with q sites. This same periodicity is also reflected in the phase θ . We take p, q as successive Fibonacci numbers

since the infinite limit $\alpha \rightarrow (\sqrt{5} - 1)/2$ is the inverse of the golden ratio, an assured irrational number. Figure 1(a) shows a schematic for $\alpha = 5/8$. For a quantum state $\Psi(n) = \phi_n$ on the lattice defined by its amplitudes at the sites n , the degree of localization is quantified by the inverse participation ratio (IPR) [14]:

$$IPR = \sum_n |\phi_n|^4 / \left(\sum_n |\phi_n|^2 \right)^2. \quad (2)$$

When the medium is localized on a single site $IPR = 1$, whereas if it is uniformly spread over all sites $IPR \rightarrow 1/q$ for a lattice with q sites, vanishing in the limit of an infinite lattice. Figure 1(b) shows a surface plot of the IPR for the ground state as a function of the modulation phase θ and the ratio $\gamma = J_2/J_1$. A top view of the same is shown in Fig. 1(d). A localization transition, as predicted by Aubry and André [7,15], is clearly visible, particularly in the top view. Since the ring is finite, the transition occurs gradually across the critical value of $\gamma = 2$, becoming sharper with increasing lattice sites.

The most striking feature evident in the figures is the dependence on the modulation phase θ in the regime $\gamma > 2$ where, although the medium is generally localized, the IPR periodically decreases sharply, indicating partial delocalization around specific values of the phase. These regimes of partial delocalization grow progressively narrower farther away from the critical point, as illustrated in a contour plot, Fig. 1(c), centered at one of the dips. An intuitive explanation is found in the limit $\gamma \gg 1$, dominated by the cosine term, which typically has a global minimum at a single site where states localize, but at the dips the minimum is shared by two sites [16].

In the infinite limit, a discrete Fourier transform $\psi_n = \sum_m \varphi_m e^{im(2\pi n\alpha)}$ gives an equation dual to Eq. (1):

$$J_2[\varphi_{m+1}e^{-i\theta} + \varphi_{m-1}e^{i\theta}] + 4J_1 \cos(2\pi\alpha m)\varphi_m = 2E\varphi_m. \quad (3)$$

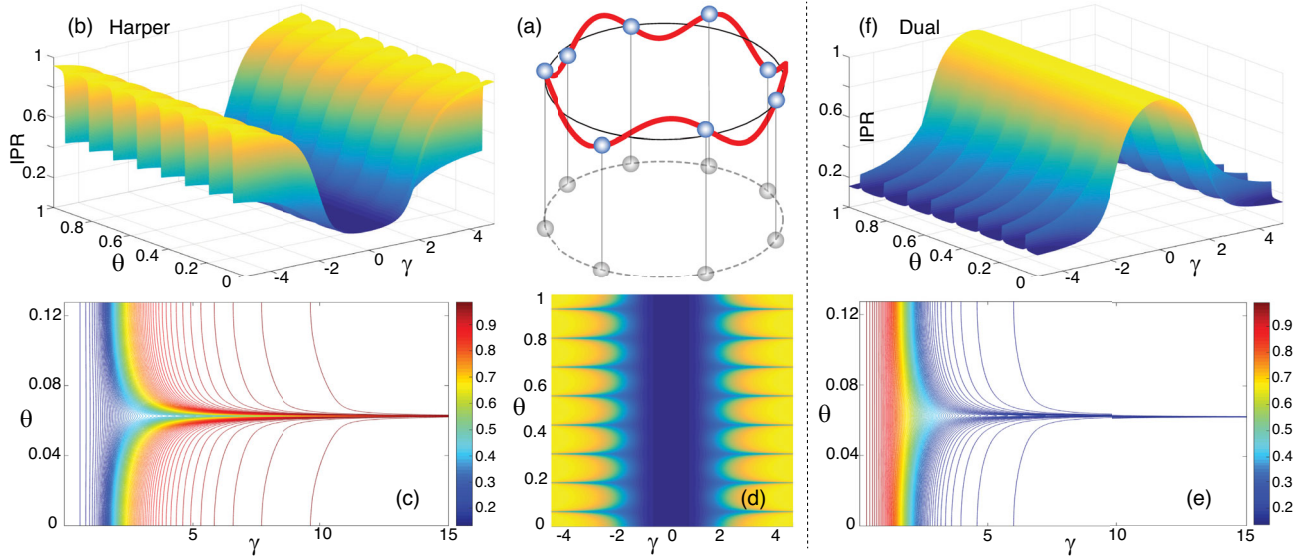


FIG. 1. Counterclockwise from top center, with θ in units of 2π in all figures. (a) Schematic of a discrete ring-shaped lattice with eight sites shown as gray circles at the bottom. Cosine modulation at a different period (five full oscillations around, shown in red) shifts the energies at the sites, with the resulting lattice shown above as blue circles (the lines are for visual guidance). (b) The ground state IPR transitions around $\gamma = J_2/J_1 = 2$ from unity, indicating localization of the medium, to a low value, indicating an extended state. But, in the localized regime, there is partial delocalization near certain values of the phase, θ , that manifests as narrow dips. (d) The top view of the same. (f) The dual Hamiltonian shows the opposite trend, the ground state IPR transitions from a value of unity for $\gamma < 2$ to a low value for $\gamma > 2$, and now there is partial localization near the same values of the phase, marked by narrow ridges in the plot. (c),(e) Top view contour plots corresponding to sections of (b) and (f), respectively, for extended values of γ showing progressive narrowing of the delocalization dips and localization ridges.

We compute the IPR for this dual Hamiltonian also on a finite ring. Figure 1(f) shows a surface plot of the ground state IPR for $\alpha = 5/8$ as a function of γ and the phase θ in the exponent. As with the Harper equation, the localization transition is evident, but the regimes are switched, consistent with predictions in the infinite limit. In the delocalized regime, sharp ridges of partial localization are conspicuous, complementary to the dips seen with Eq. (1) but similarly narrowing as γ increases, highlighted by a contour plot, Fig. 1(e), centered on a ridge.

Features.—Although we use the Fibonacci ratio, the partial (de)localization effects occur for *any* ratio p/q , but the sharpness of the ridges and dips vary. The regions of dips or ridges match the number of lattice sites, serving to visualize the magnetic period [17] that manifests as symmetry under lattice translations [12]. When the site number approaches infinity, $\alpha \rightarrow (\sqrt{5} - 1)/2$, those regions approach a zero measure as more periods squeeze into the span of $[0, 2\pi)$, consistent with theorems asserting all states are localized for $\gamma > 2$ for the Harper equation and vice versa for its dual [18,19]. The average IPR, taken over all states in the ground band, displays similar features; the case of $\alpha = 3/5$ is shown in Fig. 2(a). Additional periodic structure beyond the magnetic period arises from the excited states, evident in the cross sections of their IPR at fixed γ plotted in Fig. 2(b).

The significance of the ring structure becomes evident by contrasting it with a box boundary condition. For the

Harper equation, Eq. (1), the localization dips remain, but the regular pattern can be distorted, as seen in Fig. 2(c). However, for the dual equation, Eq. (3), the localization ridges completely *vanish* for the box boundary condition. Physically, this makes sense because the phase in the Harper equation is a relative phase of the modulation with respect to the underlying lattice; whereas the phase in the dual equation appears as an absolute phase, so only when we impose the periodic boundary condition, the single valuedness of quantum states makes that phase physically relevant, a situation analogous to that for the Berry phase [2] and the Aharonov-Bohm effect [1].

A qualitative explanation can be found in Thouless's relation [20] between localization and the spectrum, utilized by Aubry and André [7] to posit the existence of the localization transition at $\gamma = 2$. For a box boundary condition, properties of tridiagonal matrices [16,21] show that the characteristic equation for the Hamiltonian in Eq. (1) depends on the phase but is independent of it for the dual Hamiltonian in Eq. (3). But, in a ring lattice, phase dependence occurs for both cases. Indeed, in a ring, we find that the Thouless exponent for the degree of localization $\lambda_j = (q - 1)^{-1} \sum_{j \neq i} \ln |E_j - E_i|$ plotted for the Harper ground state $j = 0$ in Fig. 2(d) follows the same pattern as with the IPR. However, because the Thouless expression strictly applies to an open 1D lattice, this is only a qualitative argument to suggest that the phase dependence

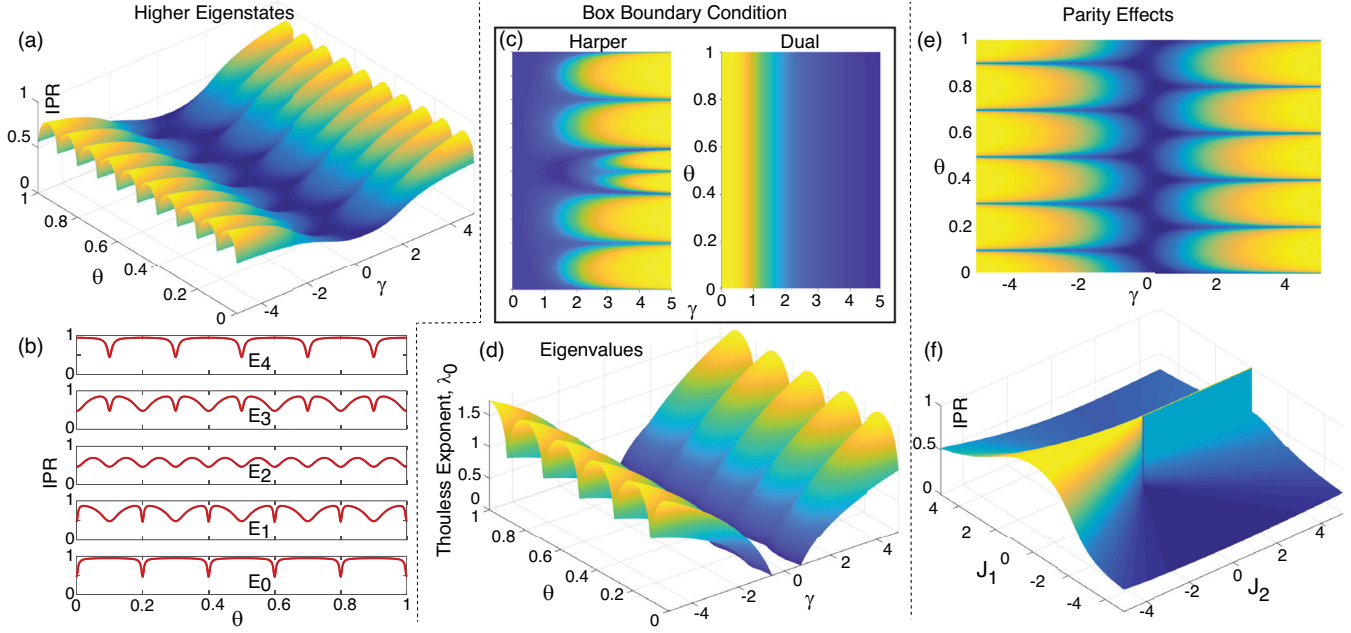


FIG. 2. Features illustrated with the discrete model for a ring lattice with $q = 5$ sites and $\alpha = 3/5$, all for the Harper equation Eq. (1) except where mentioned. (a) The IPR averaged over all states in the lowest band displays the localization transition and dependence on the phase θ as for the ground state in Fig. 1. (b) The dependence of the IPR on the phase θ at fixed $\gamma = 5$ is shown for each state in the lowest band, labeled by eigenenergies E_i in ascending value. (c) With a box boundary condition, the phase dependence of the IPR, shown for the ground state, persists for the Harper equation although distorted, but for the dual case Eq. (3) that dependence vanishes altogether. (d) Thouless exponent λ_0 for the lowest band, referenced to the ground state, displays the same phase dependence as the IPR. (e) The ground state IPR reveals an asymmetry with respect to the sign of γ . (f) This asymmetry is conspicuous when J_1 and J_2 are varied for fixed $\theta = 0$.

of the IPR arises from the spectral properties of the respective Hamiltonians.

Comparing Fig. 2(e) for $\alpha = 3/5$ with Fig. 1(d), where $\alpha = 5/8$, reveals an asymmetry under parity of γ for odd q because for J_1 fixed, $J_2 \rightarrow -J_2$ in Eq. (1) amounts to $\cos[2\pi(np/q) + \theta] \rightarrow \cos[2\pi(np + q/2)/q + \theta]$. The asymmetry highlights the IPR dips. The IPR plotted in Fig. 2(f) versus J_1 and J_2 for $\theta = 0$ reaches complete localization for $J_2 < 0$ but only partial localization for $J_2 > 0$. Changing both J_1 and J_2 reverses the order of the eigenvalues, so the ground state IPR is for the previously highest energy state in the band.

Continuum model.—Consider now a physical lattice implemented with a bichromatic potential [Fig. 3(a)]:

$$-\frac{\hbar^2}{2m} \frac{d^2}{dx^2} + V \sin^2\left(\frac{\pi x}{a}\right) + \gamma \Delta \cos\left(\frac{2\pi ax}{a} + \theta\right). \quad (4)$$

The second term creates the lattice structure of Eq. (1) and the last term, the Harper modulation. The hopping strength is estimated as $\Delta = |\langle w_n | H_0 | w_{n+1} \rangle|$ using Wannier states w_n localized at adjacent sites. H_0 neglects the relatively smaller Harper term, while γ as defined has the same role as its discrete counterpart [22]. Figure 3(b) confirms that the IPR computed for this Hamiltonian has the same features as

the discrete model, including the localization transition and the sharp θ -periodic dips.

In the continuum counterpart of the dual Hamiltonian Eq. (3), the effect of the phase in the coupling appears as a minimally coupled gauge potential, Ω [16]:

$$\gamma \left[\frac{1}{2m} \left(-i\hbar \frac{d}{dx} - \Omega \right)^2 + V \sin^2\left(\frac{\pi x}{a}\right) \right] + 4\Delta \cos\left(\frac{2\pi ax}{a}\right). \quad (5)$$

The Ω^2 term has no impact on the IPR, so the kinetic term in Eq. (5) can be reduced to $\gamma[-(\hbar^2/2m)(d^2/dx^2) + i(\hbar/m)\Omega(d/dx)]$ and Ω interpreted as the angular velocity for unit ring radius r [22]. We assume $\hbar = m = e = r = 1$. The ground state IPR for this Hamiltonian in Fig. 3(c) displays localization transition and localization ridges, now as function of Ω . The γ parity effect is more pronounced here because the computed spectrum includes multiple bands, and as all eigenvalues reorder, the “ground state” IPR for $+\gamma$ and $-\gamma$ corresponds to states from different bands.

Sensing by localization.—The strong phase dependence displayed by the IPR offers a novel alternate principle for sensors based on localization transition. Since the results rely only upon assuming a ring system, a dual periodic potential, and wavelike behavior, the principle can find broad applications. Here, we mention a few.

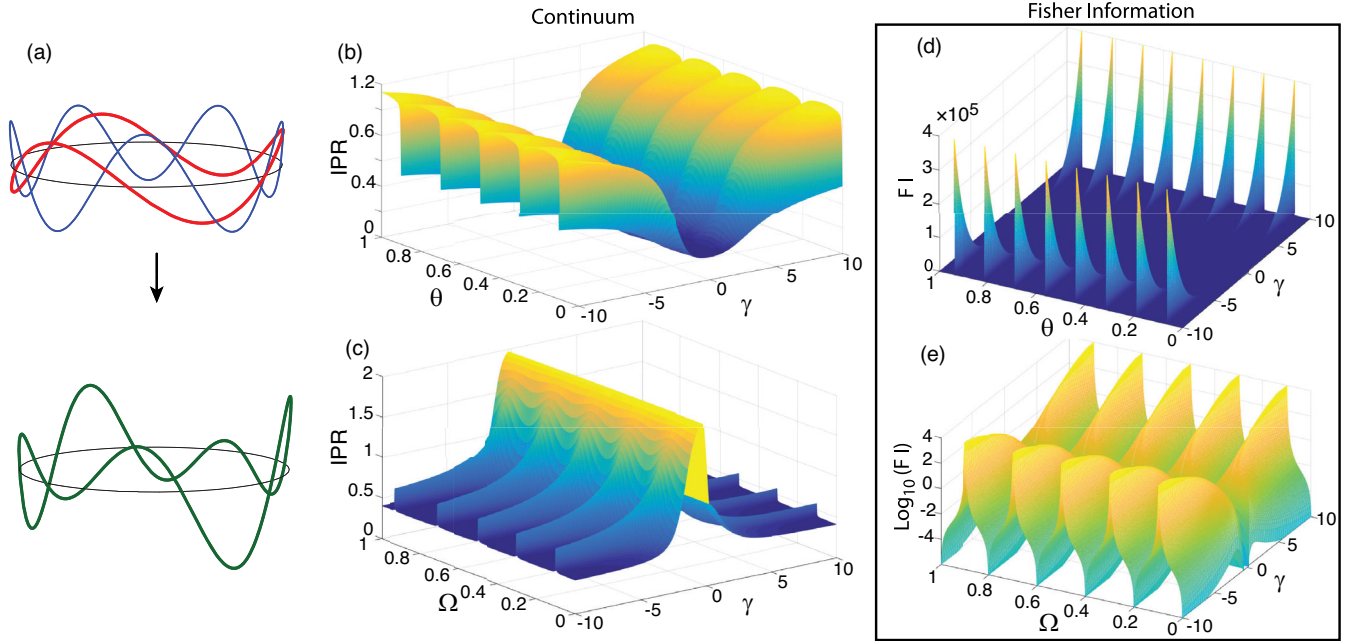


FIG. 3. (a) Schematic of the continuum model with two sinusoidal potentials of commensurate periodicities, $p = 3$ and $q = 5$, in a ring with $\alpha = 3/5$. (b) The IPR computed with Hamiltonian Eq. (4) displays behavior analogous to its discrete counterpart [Fig. 2(e)] with matching narrow dips. (c) The continuum dual Hamiltonian, Eq. (5), also reproduces the behavior of its discrete counterpart, with localization ridges now as function of gauge potential Ω (units of $2\pi/a$), occurring in the extended regime $\gamma > 2$. (d) The Fisher information plotted for the discrete Harper equation, Eq. (1), displays high sensitivity to the phase θ at the location of the dips in the IPR. (e) Sensitivity to Ω also spikes at the position of the partial localization ridges for the continuum dual Hamiltonian, Eq. (5), but the log scale reveals more structure.

The continuum ring Hamiltonian in Eq. (5) can be implemented with ultracold atoms in a ring-shaped lattice [23] with two overlapping commensurate periodicities, building on current capabilities with ring traps. The system can be calibrated to match $\Omega = 0$ with a localization ridge such that a slight rotation will induce a significant change in the degree of localization of the medium. Calibration to an offset from a maximum will allow determination of directionality. Alternately, the component lattices can be linked to two independent systems; then the change in the phase θ in Eq. (4) can measure relative rotation or torsion via the localization dips.

In a separate application, with Ω interpreted as the vector potential, this same principle can be used for precision sensing of magnetic fields using a charged medium in a ring formed, for instance, with coupled quantum wells with cosine modulation of their on-site energies [24].

We quantify the sensitivity of such sensor applications with the Fisher information (FI) for the probability distribution function $P(x; \phi)$ along the ring as follows:

$$FI = \int dx P(x; \phi) [\partial_\phi \ln P(x; \phi)]^2, \quad (6)$$

with observable $\phi \equiv \Omega$ for the continuum, and $\phi \equiv \theta$ and the integral replaced by a sum over sites for a discrete

lattice. In Fig. 3(d), the FI for the ground state distribution for the discrete Harper equation, Eq. (1), displays heightened sensitivity to θ along the IPR dips, rising with γ . Likewise, sensitivity to Ω spikes in Fig. 3(e) along the ridges for the ground state IPR for the continuum dual Hamiltonian, Eq. (5), with more detailed structure revealed by the semilog plot. Both demonstrate that high sensitivity can be achieved, benchmarked for instance by $FI \sim 4\pi^2$, for Sagnac interferometry on a ring [25].

Effect of interactions.—Ultracold atoms in lattices typically have interparticle interactions. We assessed their effects by considering a Bose-Hubbard Hamiltonian [26,27] adapted to the Harper equation, Eq. (1), and its dual Eq. (3) [16]. We examined both cases with different numbers of lattice sites q and particles N , computing the many-body ground state wave function Φ_0 and the associated single particle density matrix $\rho_{ij} = \langle \Phi_0 | \hat{a}_i^\dagger \hat{a}_j | \Phi_0 \rangle$. We evaluated the IPR in two separate ways: (i) by inserting the components of Φ_0 in Eq. (2) and (ii) by substituting $|\phi_n|^2 \rightarrow \rho_{nn}$, the diagonal elements of the single particle density matrix. Without interactions, $U = 0$, the IPRs demonstrate all the features described above, including the localization transition and the dips and ridges [examples for the dual case are shown in Fig. 4(a),(b)]. The phase dependent dips and ridges were present regardless of whether or not N and q were mutually commensurate.

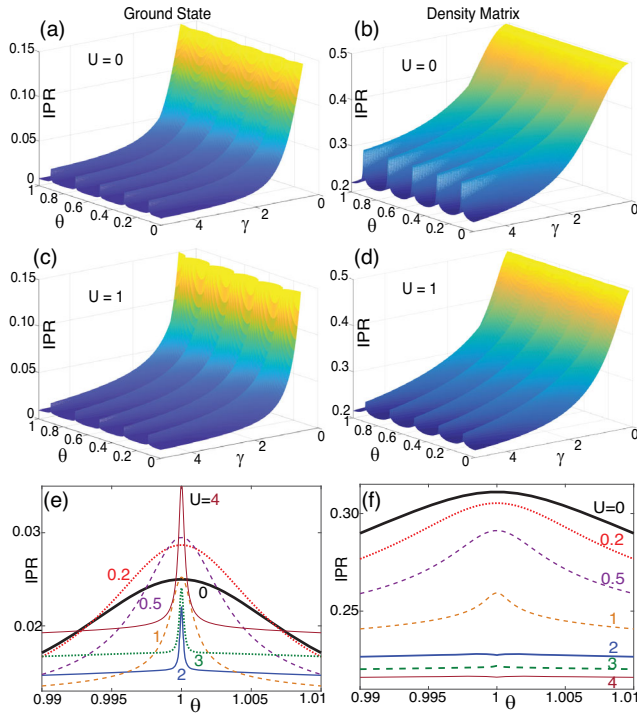


FIG. 4. The Bose-Hubbard model [16] is used to simulate effects of interparticle interactions in the dual case, shown here for $N = 7$ particles in $q = 5$ sites for $\alpha = 3/5$. The left panels compute the IPR with the ground state and the right panels utilize the single particle density matrix. (a),(b) The IPR computed with no interaction, $U = 0$. (c),(d) The IPR computed with interaction $U = 1$. (e),(f) The line plots display how the sharpness of a partial localization ridge varies with the interaction strength U at fixed $\gamma = 4$.

Interactions make the ridges less prominent, as seen in Fig. 4(c),(d). However, the decline is not monotonic, as seen in Fig. 4(e),(f), which plots the IPR around one of the localization ridges for fixed γ . The many-body ground state IPR shows sharpening of the ridge with increasing U before broadening out, suggesting rich nonlinear effects we continue to study.

Outlook.—Several lines of further investigation are indicated, spanning basic research that includes rigorous analysis of localization in finite rings, effects of time evolution and interactions, and applied research on experimental implementation [28,29] and in metrology.

We gratefully acknowledge discussions with Prof. D. Schneble and the support of the NSF under Grant No. PHY-1707878.

-
- [1] Y. Aharonov and D. Bohm, Significance of electromagnetic potentials in the quantum theory, *Phys. Rev.* **115**, 485 (1959).
 [2] M. V. Berry, Quantal phase factors accompanying adiabatic changes, *Proc. R. Soc. A* **392**, 45 (1984).

- [3] B. D. Josephson, The discovery of tunnelling supercurrents, *Rev. Mod. Phys.* **46**, 251 (1974).
 [4] P. G. Harper, Single band motion of conduction electrons in a uniform magnetic field, *Proc. Phys. Soc.* **68**, 874 (1955).
 [5] D. R. Hofstadter, Energy levels and wave functions of Bloch electrons in rational and irrational magnetic fields, *Phys. Rev. B* **14**, 2239 (1976).
 [6] D. J. Thouless, M. Kohmoto, M. P. Nightingale, and M. den Nijs, Quantized Hall Conductance in a Two-Dimensional Periodic Potential, *Phys. Rev. Lett.* **49**, 405 (1982).
 [7] S. Aubry and G. André, Analyticity breaking and Anderson localization in incommensurate lattices, *Ann. Isr. Phys. Soc.* **3**, 133 (1980).
 [8] H. Miyake, G. A. Siviloglou, C. J. Kennedy, W. C. Burton, and W. Ketterle, Realizing the Harper Hamiltonian with Laser-Assisted Tunneling in Optical Lattices, *Phys. Rev. Lett.* **111**, 185302 (2013).
 [9] M. Aidelsburger, M. Atala, M. Lohse, J. T. Barreiro, B. Paredes, and I. Bloch, Realization of the Hofstadter Hamiltonian with Ultracold Atoms in Optical Lattices, *Phys. Rev. Lett.* **111**, 185301 (2013).
 [10] J. Dalibard, F. Gerbier, G. Juzeliūnas, and P. Öhberg, Colloquium: Artificial gauge potentials for neutral atoms, *Rev. Mod. Phys.* **83**, 1523 (2011).
 [11] N. Goldman, G. Juzeliūnas, P. Öhberg, and I. B. Spielman, Light-induced gauge fields for ultracold atoms, *Rep. Prog. Phys.* **77**, 126401 (2014).
 [12] P. Marra, R. Citro, and C. Ortix, Fractional quantization of the topological charge pumping in a one-dimensional superlattice, *Phys. Rev. B* **91**, 125411 (2015).
 [13] X. Ni, K. Chen, M. Weiner, D. J. Apigo, C. Prodan, A. Alù, E. Prodan, and A. B. Khanikaev, Observation of Hofstadter butterfly and topological edge states in reconfigurable quasi-periodic acoustic crystals, *Commun. Phys.* **2**, 55 (2019).
 [14] B. Kramer and A. MacKinnon, Localization: Theory and experiment, *Rep. Prog. Phys.* **56**, 1469 (1993).
 [15] M. Ya. Azbel, Quantum Particle in One-Dimensional Potentials with Incommensurate Periods, *Phys. Rev. Lett.* **43**, 1954 (1979).
 [16] See Supplemental Material at <http://link.aps.org/supplemental/10.1103/PhysRevLett.125.070401> for more details on (i) explanation of the phase dependence of the spectrum based on features of relevant characteristic equations, (ii) intuitive explanation for the localization dips appearing as a function of the phase, (iii) the Bose-Hubbard equations used, (iv) the relation between the coupling phase in the dual Hamiltonian and gauge potentials.
 [17] J. Zak, Magnetic translation group, *Phys. Rev.* **134**, A1602 (1964).
 [18] S. Ya. Jitomirskaya, Metal-insulator transition for the almost Mathieu operator, *Ann. Math.* **150**, 1159 (1999).
 [19] J. Avron and B. Simon, Singular continuous spectrum for a class of almost periodic Jacobi matrices, *Bull. Am. Math. Soc.* **6**, 81 (1982).
 [20] D. J. Thouless, A relation between the density of states and range of localization for one dimensional random systems, *J. Phys. C* **5**, 77 (1972).

-
- [21] L. G. Molinari, Determinants of block tridiagonal matrices, *Linear Algebra Appl.* **429**, 2221 (2008).
- [22] K. K. Das and J. Christ, Realizing the Harper model with ultracold atoms in a ring lattice, *Phys. Rev. A* **99**, 013604 (2019).
- [23] S. Franke-Arnold, J. Leach, M. J. Padgett, V. E. Lembessis, D. Ellinas, A. J. Wright, J. M. Girkin, P. Öhberg, and A. S. Arnold, Optical ferris wheel for ultracold atoms, *Opt. Express* **15**, 8619 (2007).
- [24] D. Ferry, S. M. Goodnick, and J. Bird, *Transport in Nanostructures*, 2nd ed. (Cambridge University Press, UK, 2009).
- [25] S. A. Haine, Mean-Field Dynamics and Fisher Information in Matter Wave Interferometry, *Phys. Rev. Lett.* **116**, 230404 (2016).
- [26] M. P. A. Fisher, P. B. Weichman, G. Grinstein, and D. S. Fisher, Boson localization and the superfluid-insulator transition, *Phys. Rev. B* **40**, 546 (1989).
- [27] D. Jaksch, C. Bruder, J. I. Cirac, C. W. Gardiner, and P. Zoller, Cold Bosonic Atoms in Optical Lattices, *Phys. Rev. Lett.* **81**, 3108 (1998).
- [28] M. Lohse, C. Schweizer, O. Zilberberg, M. Aidelsburger, and I. Bloch, A Thouless quantum pump with ultracold bosonic atoms in an optical superlattice, *Nat. Phys.* **12**, 350 (2016).
- [29] S. Nakajima, T. Tomita, S. Taie, T. Ichinose, H. Ozawa, L. Wang, M. Troyer, and Y. Takahashi, Topological Thouless pumping of ultracold fermions, *Nat. Phys.* **12**, 296 (2016).